

Article

Vibrational Dynamics of Crystalline 4-Phenylbenzaldehyde from INS Spectra and Periodic DFT Calculations

Mariela M. Nolasco ^{1,*}, Catarina F. Araujo ¹, Pedro D. Vaz ², Ana M. Amado ³ and Paulo Ribeiro-Claro ¹

¹ CICECO, Departamento de Química, Universidade de Aveiro, P-3810-193 Aveiro, Portugal; catarina.araujo@ua.pt (C.F.A.); prc@ua.pt (P.R.-C.)

² Champalimaud Foundation, Champalimaud Centre for the Unknown, 1400-038 Lisboa, Portugal; pedro.vaz@fundacaochampalimaud.pt

³ Química-Física Molecular, Departamento de Química, FCTUC, Universidade de Coimbra, P-3004-535 Coimbra, Portugal; amado.am@gmail.com

* Correspondence: mnolasco@ua.pt; Tel.: +351-234-370-360

Received: 24 February 2020; Accepted: 16 March 2020; Published: 18 March 2020



Abstract: The present work emphasizes the value of periodic density functional theory (DFT) calculations in the assessment of the vibrational spectra of molecular crystals. Periodic calculations provide a nearly one-to-one match between the calculated and observed bands in the inelastic neutron scattering (INS) spectrum of crystalline 4-phenylbenzaldehyde, thus validating their assignment and correcting previous reports based on single molecule calculations. The calculations allow the unambiguous assignment of the phenyl torsional mode at ca. 118–128 cm⁻¹, from which a phenyl torsional barrier of ca. 4000 cm⁻¹ is derived, and the identification of the collective mode involving the antitranslational motion of CH...O bonded pairs, a hallmark vibrational mode of systems where C-H...O contacts are an important feature.

Keywords: inelastic neutron scattering; density functional theory; vibrational assignment; molecular crystal; torsional potential; C-H...O hydrogen bonds

1. Introduction

The use of periodic density functional calculations (periodic DFT) to address the vibrational spectra of molecular crystals is becoming increasingly popular [1–12]. In fact, the periodic DFT approach, although originally developed to deal with extended inorganic systems, was found to be highly efficient in predicting the vibrational spectra of molecular crystals [13]. Periodic methods—available through programs such as VASP [14], CRYSTAL [15,16] and CASTEP [17]—are often used to assist vibrational assignments of infrared and inelastic neutron scattering (INS) spectra of molecular crystals [1,2,6–9,18]. Vibrational spectroscopy with neutrons provides information not accessible from the optical techniques (IR and Raman), due to the absence of selection rules. The relationship between periodic DFT calculations and INS spectroscopy is somewhat synergistic. The intensity of INS bands is proportional to the relative atomic displacements in normal modes [19], which, in turn, are a straightforward result of the computational approach to vibrational frequencies. The ability of periodic calculations to predict INS intensities with high accuracy leads to mostly unambiguous assignments of vibrational modes and, additionally, provides the means to test the validity of the molecular model used [6,20].

The crystal structure of 4-phenylbenzaldehyde has been addressed in a comprehensive crystallographic, spectroscopic and computational study of C-H...O hydrogen bonds [21]. More recently, the complete assignment of infrared and Raman spectra has been proposed based on discrete

DFT calculations [22]. These works try to describe the vibrational spectra of the crystal through discrete calculations, either by choosing the simpler and most common “isolated molecule” approach [22] or by using several “dimer associations” to represent the possible interactions in the crystal [21]. Hence, 4-phenylbenzaldehyde is a suitable subject to test the “computational spectroscopy” approach to molecular crystals using periodic calculations. By combining periodic DFT calculations with INS spectra it is possible to validate assignments and assess vibrational dynamics of 4-phenylbenzaldehyde in the crystal.

2. Results and Discussion

2.1. Molecular Geometry and Intermolecular Interactions

Figure 1 presents a fragment of the crystal structure of 4-phenylbenzaldehyde, along with the numbering scheme adopted in this work. The crystal structure (monoclinic, space group $P21/a$, $Z = 4$) [21] is built from two types of dimers: the C-H \cdots O bonded dimers (molecules labeled A) coexist with pi-stacking dimers (molecules labeled B), as shown in Figure 1. All molecules are involved in both types of dimers, but they have slightly different secondary neighboring contacts.

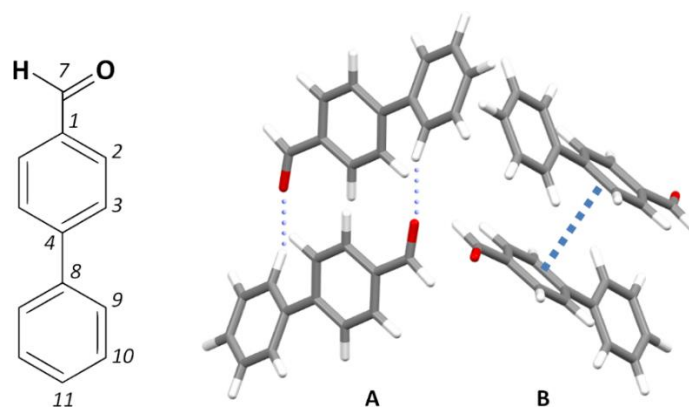


Figure 1. Representation of 4-phenylbenzaldehyde, with the atom labeling used throughout the text (left) and fragment of the crystal structure, evidencing the two types of dimer present in the crystal (right) [21].

Table 1 compares some selected geometrical parameters obtained from X-ray [21], periodic calculations (CASTEP, see experimental details) and discrete single molecule calculations (G09, see experimental details). The “single molecule” model was chosen to perform the discrete calculations as it remains, despite its known limitations, a popular approach. The “dimer” model is not a straightforward option, due to the presence of different intermolecular contacts with identical strength (C-H \cdots O and pi-stacking, dimers A and B in Figure 1). The alternative use of a “cluster” of molecules poses two main problems: the large number of molecules required to mimic the periodic crystal motif and the erratic behavior of the outer shell of the cluster (bound by weak intermolecular forces). In the past, a method based on the sum of pairwise contributions has been used as a less computationally demanding alternative to the cluster model [23–25] but with limited advantages.

There is a good agreement between experimental and calculated crystal structures (X-ray vs. CASTEP). The root mean square deviation between Cartesian coordinates of all atoms, excluding hydrogen atoms, is less than 5%, and RMS deviation in bond lengths, excluding C-H bonds, is less than 2%. Nevertheless, CASTEP geometrical parameters present some well-known limitations of PBE calculations. The C=O bond length is clearly overestimated—leading to the underestimation of the C=O stretching mode, already discussed elsewhere [2,8]—and the pi-stacking distance evidences the expected bias to large values: this distance would deviate to physically meaningless values if not constrained by cell dimensions [2].

Table 1. Selected geometrical parameters of 4-phenylbenzaldehyde (molecules in dimers A and B).

	X-ray (A)	X-ray (B)	CASTEP(A)	CASTEP(B)	G09
<i>Bond length/pm</i>					
C7=O	118.1	118.7	122.7	122.8	120.6
C4-C8	149.2	145.5	147.8	147.8	147.7
C1-C7	148.7	148.4	146.8	146.8	147.4
<i>Dihedral angle/°</i>					
C2C1-C7O	−1.95	−2.06	−2.16	−2.26	−0.10
C3C4-C8C9	31.9	31.6	32.6	31.0	38.9
<i>Distance/pm</i>					
C9(H)⋯O	341	361	333.7	348.1	-
$\pi\cdots\pi$ (C1⋯C4') ¹	414.7	411.1	418.5	418.1	-

¹ Distance between C1 and C4 atoms of the π -stacking molecules.

The geometry of the single molecule obtained from discrete calculations (G09) at the PBE1PBE/6-311G(d,p) level (Table S1, Supplementary Materials) is in good agreement with the one recently reported at the B3LYP/6-311++G(d,p) level [22] and does not present large deviations from the CASTEP geometry. Table 1 also evidences the effect of crystal packing on the dihedral angles of aldehyde and phenyl groups. For the isolated molecule, the CHO group is predicted to be nearly coplanar with the ring, while the non-planarity between the two rings is heightened relative to the packed molecules.

2.2. Calculated vs. Experimental Spectra

Figure 2, top line, presents the experimental INS spectrum of 4-phenylbenzaldehyde (TOSCA), in the 25–1800 cm^{-1} range. Figure 2, middle and bottom lines, show the simulated INS spectra obtained from periodic (CASTEP) and discrete (G09) calculations, respectively.

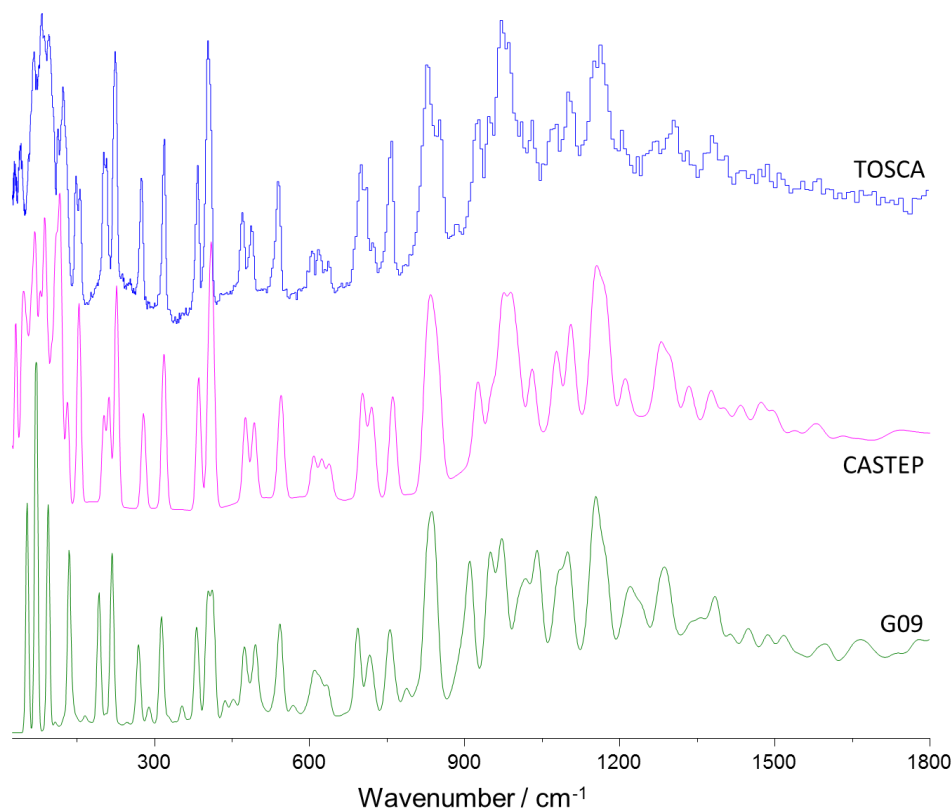


Figure 2. The inelastic neutron scattering (INS) spectra of 4-phenylbenzaldehyde in the 25–1800 cm^{-1} range: experimental (top), simulated from periodic calculations (middle) and from single molecule discrete calculations (bottom).

The immediate impression from Figure 2 is the excellent agreement between the experimental spectrum and the one estimated from periodic calculations, with a remarkable nearly one-to-one correspondence between the bands, in both their positions and intensities. As for the spectrum simulated using the single molecule approach (Figure 2, bottom), the correlation was quite satisfactory for some regions, but with clear overall limitations. For instance, there were a few “extra” bands spread in the simulated spectrum, without correspondence in the experimental spectrum, and the description of the region 900–1200 cm^{-1} was poor. Additionally, of course, the calculated spectrum for a single molecule was meaningless in the region where the contributions from collective modes were expected to prevail (ca. $<200 \text{ cm}^{-1}$).

As stated above, the excellent description of the INS spectrum obtained from periodic calculations provided a straightforward validation of the model and allowed a trustful assignment of vibrational modes of crystalline 4-phenylbenzaldehyde. The full assignment of the INS bands based on the periodic calculations is presented in Table 2. The vibrational assignment of IR and Raman spectra of 4-phenylbenzaldehyde has been performed recently, based on discrete calculations at the B3LYP/6-311++G(d,p) level [22]. Although there is a general concordance between assignments, the INS spectrum allows the clarification of some spectral features, as discussed below.

Table 2. Observed (TOSCA) and calculated (CASTEP) INS wavenumbers of 4-phenylbenzaldehyde.

CASTEP ¹	Observed	Approx. Description
3104	3030	ν C-H
1379	1384	β C7-H
1298	1312	β C-H
1170	1164	β C-H
1106	1108	β C-H
1077	1075	β C-H
1030	1032	β C-H
994	994	γ C7-H
975	973	γ C-H
953	951	γ C-H
926	929	γ C-H
845	855	γ C-H
833	832	ν C-C
762	762	γ C-H
720	715	δ ring
702	702	δ ring
638	641	α ring
622	623	β C=O
609	610	α ring
545	545	δ ring
493	493	α ring
476	475	δ ring
408	408	δ ring
385	388	β C8-C4
317	324	γ C8-C4
278	281	α ring
225	229	γ C-CHO
210-201	212-207	β C-CHO
153	152-162	τ -CHO
130	136	β C4-C8
109-117	118-128	τ -C ₆ H ₅
89	101	Libration (Ia)
67	86	Librations (Ic, Ib)
48	70	Translation (b,c)
37	45	Translation(a)

¹ Maxima in the INS simulated spectrum. ν , α , β , γ and τ stand for stretching, in-plane deformation, out-of-plane deformation and torsion modes, respectively. Librations around the molecular axes of inertia, translations along cell axes.

The 4-phenylbenzaldehyde crystal presents 192 atoms in the crystallographic unit cell (24 atoms per isolated molecule) [21], from which 573 optical modes are predicted. These include 8×66 normal vibrational modes of the eight molecules ($132A_g + 132A_u + 132B_g + 132B_u$) and 45 external modes describing translations and rotations (21 translational modes plus 24 librational modes, $12A_g + 11A_u + 11B_g + 11B_u$).

The 66 normal modes of vibration of each individual molecule include 60 related with the two phenyl rings. The “approximate description” of the normal modes in Table 2—obtained from the visualization of atomic displacements—is in accordance with the conventional notation for substituted aromatic rings: 23 stretching modes (labeled ν), 18 in-plane deformation modes (labeled α ring and β) and 18 out-of-plane deformation modes (labeled δ ring and γ). In addition, there is one torsional inter-ring mode, (τ -C₆H₅) and six modes related to the aldehyde group (ν C7=O, ν C7-H, β C7=O, β C7-H, γ C7=O and γ C7-H, one of which is in fact the torsional mode, τ -CHO). This notation keeps the traditional separation between the “in-plane” and “out-of-plane” ring modes and assumes no significant interaction between internal and external modes. This latter assumption is expected to hold for systems with weak intermolecular binding [4], as it is the case of 4-phenylbenzaldehyde. However, the same is not true for the separation between “in-plane” and “out-of-plane” modes. Since the two aromatic rings are not coplanar, there is no molecular symmetry plane and the coupling between oscillators leads to normal modes of a hybrid nature. Figure 3 illustrates the case for the mode at ca. 832 cm^{-1} . This mode is assigned to the ν C-C stretching mode of the benzaldehyde ring (carbon and hydrogen atoms move in the same direction), but the contribution from the out-of-plane γ CH modes is evident in the phenyl substituent ring (carbon and hydrogen atoms move in opposite directions).

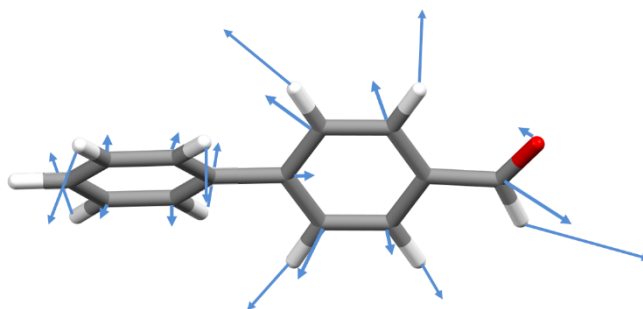


Figure 3. Atomic displacements of the normal mode at ca. 832 cm^{-1} , assigned to a ν C-C stretching mode of the benzaldehyde ring.

The assignments in Table 2 can be compared with the ones recently reported [22]. The out-of-plane deformation mode of the aldehyde CH (γ C7-H) was clearly assigned to the intense INS band at 990 cm^{-1} , while the band at ca. 1030 cm^{-1} was ascribed to the ring CH bending modes (β C-H). The mode at 832 cm^{-1} was better described as ring stretching (ν CC), despite its mixed nature, as described above. The contribution of ring deformation to the 623 cm^{-1} mode was high, but not more important than the C1-C7=O bond angle deformation, and thus the band was assigned to β C=O. This bending mode has been misassigned to the band at 475 cm^{-1} [22], which is, in fact, an out-of-plane deformation of the ring (δ ring). For the remaining low-wavenumber modes, the distinct description of the normal modes may arise from their complex mixture, which hampers the identification of the most relevant contribution in each case. This is an acknowledged limitation of the “approximate description” of the normal modes, chosen in favor of simplicity, as discussed elsewhere [2]. The exception is the inter-ring torsional mode (labeled phenyl torsion, τ -C₆H₅), which is unambiguously found to occur at much higher energy (ca. 109 – 115 cm^{-1}) than predicted from discrete calculations.

2.3. Large Amplitude, Low Wavenumber Motions

One of the major advantages of INS spectroscopy is to afford rich information in the low wavenumber region, providing a glimpse into the molecular dynamics of the systems. Both large amplitude molecular (internal) modes and crystal lattice collective (external) modes present a strong intensity in the INS spectrum, mainly due to the large displacements of hydrogen atoms. Figure 4 compares the Raman, IR and INS spectra of crystalline 4-phenylbenzaldehyde in the region below 450 cm^{-1} , evidencing the richness of the INS spectrum.

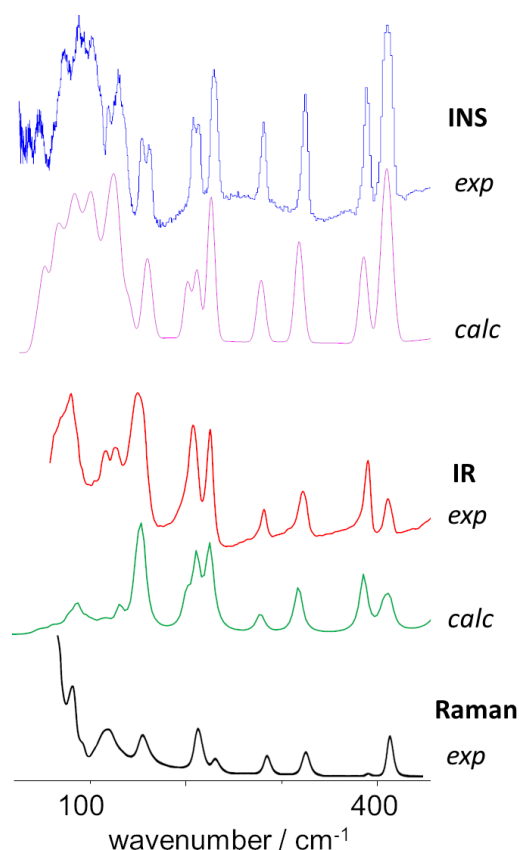


Figure 4. Vibrational spectra of 4-phenylbenzaldehyde in the spectral region below 450 cm^{-1} . From top to bottom: INS spectra (experimental, calculated), far-infrared spectra (experimental, calculated) and Raman spectrum (experimental).

As stated above, there is little interaction between internal and external modes in 4-phenylbenzaldehyde, which is consistent with a crystal packing based on C-H \cdots O and pi-stacking weak interactions. In this way, it is still plausible to describe the large amplitude/low wavenumber modes in terms of internal vibrations of the molecules vs. collective motions.

Among the most relevant internal low-wavenumber modes there are the torsional motions of the aldehyde and phenyl groups ($-\text{CHO}$ and C_6H_5- , respectively). The torsion of the $-\text{CHO}$ group is predicted to be at ca. $148\text{--}153\text{ cm}^{-1}$ from periodic calculations (CASTEP) and at ca. 139 cm^{-1} from discrete calculations (G09). This latter value compares with the one obtained from similar discrete calculations at the B3LYP level (133 cm^{-1} [22]).

As it can be seen in Figure 4, the calculated INS wavenumbers for $-\text{CHO}$ torsion merge into a single band when assuming a reasonable linewidth. Nevertheless, the predicted band matches with the doublet found at ca. $152\text{--}162\text{ cm}^{-1}$, providing an unambiguous assignment. This value of the torsional frequency is above the value reported for the 4-fluorobenzaldehyde crystal (120 cm^{-1} [4]), and suggests a somewhat stronger restriction of the CHO group dynamics in 4-phenylbenzaldehyde.

The potential energy function for internal rotation is generally described by the sum of cosine terms,

$$V(\theta) = \frac{1}{2} \sum_n V_n (1 - \cos n\theta) \quad (1)$$

from which the energy levels for torsional motion can be derived by solving the Hamiltonian for the internal rotor. More usefully, the barrier height can be estimated by fitting the energy level differences to the observed torsional transitions [26].

For the isolated molecule, the internal rotation potential obtained from discrete calculations (G09) can be described by the V_2 component, $V_2 = 3600 \pm 100 \text{ cm}^{-1}$ ($42.6 \pm 1.3 \text{ kJ/mol}$), consistent with the calculated torsional frequency of ca. 139 cm^{-1} . This barrier height is in line with the one determined for benzaldehyde molecule from different quantum chemical calculations (ca. $V_2 = 2700\text{--}2900 \text{ cm}^{-1}$) [27]. For the crystalline state, the experimental value of 153 cm^{-1} can be obtained from a V_2 barrier of nearly $4000 \pm 100 \text{ cm}^{-1}$, ($47.8 \pm 1.3 \text{ kJ/mol}$, see Figure 5, top panel). Even though the assumption of a pure V_2 barrier in the crystal is a crude approximation, it suggests that the internal rotation dynamics of the $-\text{CHO}$ group is mainly determined by intramolecular properties. The intermolecular interactions resulting from crystal packing represent a modest barrier height increase of ca. 5.2 kJ/mol , which is consistent with the presence of weak $\text{CH}\cdots\text{O}$ interactions [21].

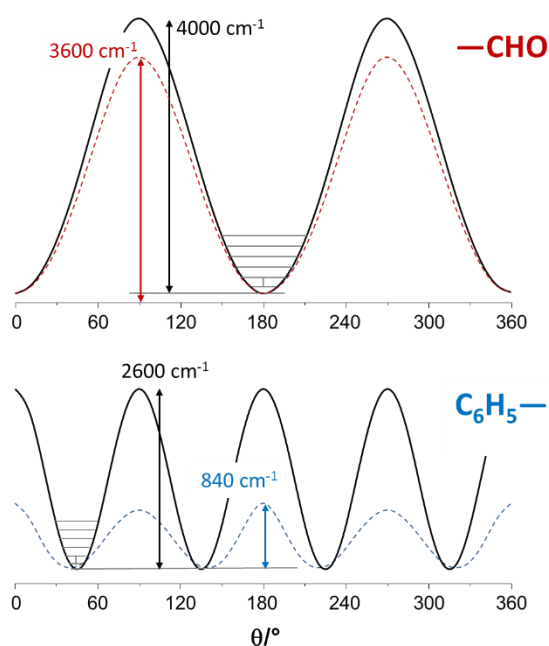


Figure 5. Potential curves for internal rotation of $-\text{CHO}$ (top) and C_6H_5- (bottom) groups in 4-phenylbenzaldehyde. Dashed lines from single molecule calculations (G09, energy vs. dihedral angle), solid lines from experimental wavenumber in the crystal (Barrier [26]). The G09 potential curve for phenyl internal rotation (blue dashed line) is described by the terms $V_2 = -241 \text{ cm}^{-1}$, $V_4 = 743 \text{ cm}^{-1}$, $V_6 = 126 \text{ cm}^{-1}$ and $V_8 = 51 \text{ cm}^{-1}$.

As for the torsion of the phenyl substituent (C_6H_5-), the effect of crystal packing is more pronounced. In fact, discrete calculations (G09) yield a torsional frequency value of only ca. 70 cm^{-1} , while periodic calculations yield split torsional frequencies of $109\text{--}117 \text{ cm}^{-1}$. Similar G09 calculations [22] lead to the assignment of phenyl torsion to a Raman band at ca. 65 cm^{-1} . However, comparison between calculated and observed INS spectra in Figure 4 clearly suggests the assignment of the phenyl torsional mode in the crystal to the bands at ca. $118\text{--}128 \text{ cm}^{-1}$, while the INS band at ca. 70 cm^{-1} is better ascribed to a collective “external” mode (Table 2). It should be mentioned that a phenyl torsion frequency of ca

116 cm^{-1} was recently identified in an ethylene terephthalate polymer (PET) from INS and CASTEP calculations [28].

The inter-ring torsional potential for the isolated molecule (G09) is dominated by a V_4 component, with significant contributions from V_2 , V_6 and V_8 (Figure 5, bottom panel). However, the calculated torsional frequency of 70 cm^{-1} can be obtained from a simplified approach, assuming a pure V_4 term of ca. $860 \pm 30\text{ cm}^{-1}$ ($10.3 \pm 0.3\text{ kJ/mol}$). Within the same approximation, the observed frequency of 128 cm^{-1} for the crystal corresponds to a V_4 barrier of $2600 \pm 80\text{ cm}^{-1}$. The large difference indicates that, in this case, the barrier to internal rotation is mainly dominated by the intermolecular contacts—most probably the steric hindrance resulting from crystal packing, which is expected to be significant for a large group such as the phenyl group. The reports on the torsional barrier for the phenyl group are scarce, but there is a tendency for a pronounced increase from the gas phase to the condensed phase, as shown in Table 3.

Table 3. Comparison of V_4 values for internal rotation of phenyl group derived from experiment.

System		V_4/cm^{-1}	Ref.
4-phenylbenzaldehyde	INS, crystal	2600 ± 80	This work
Biphenyl	Raman, crystal	2650–200	[29]
Anisole	Raman, crystal	4033	[30]
Trans-Stilbene	Fluorescence, supersonic jet	1550	[31]
4-Methoxy-stilbene	Fluorescence, supersonic jet	1430	[32]

The 45 external modes of the crystallographic unit cell give rise to a limited number of bands in the low wavenumber region. Table 2 identifies the four main bands observed in this region, and Figure 6 presents the atomic displacements of some external modes with relevant contributions to these bands. Of course, there are several other combinations of translational and librational motions accounting for the final intensities of the four bands.

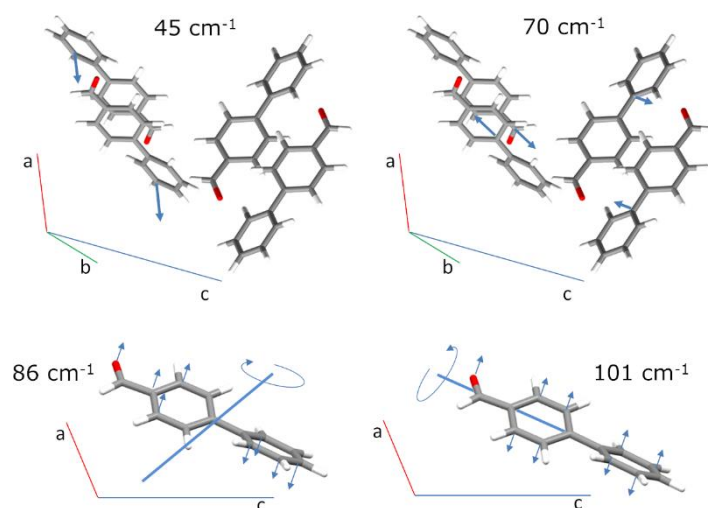


Figure 6. Schematic representation of atomic displacements for the external modes at 45 cm^{-1} , 70 cm^{-1} (translations), 86 cm^{-1} and 101 cm^{-1} (librations). For better readability, only the total displacement of the molecules is shown for translations and only the displacements of heavy atoms are shown for librations.

The translational mode at 70 cm^{-1} deserves particular discussion. As depicted in Figure 6, the full displacement of the molecules in this external mode results in the “slipping” between pi-stacked molecules, and the “antitranslational” motion of the $\text{CH}\cdots\text{O}$ bonded molecules. This antitranslational mode, which in fact represents the stretching vibration of the $\text{H}\cdots\text{O}$ intermolecular hydrogen

bond ($\nu_{\text{H}\cdots\text{O}}$), has been identified in other systems through INS spectroscopy [33–36]. In the chloroform–acetone complex this mode has been ascribed to the INS band at ca. 82 cm^{-1} [33]. More interestingly, cyclopentanone dimers—with a symmetric double $\text{CH}\cdots\text{O}$ contact, as found for 4-phenylbenzaldehyde dimer—present the anti-translational mode at 95 cm^{-1} [34]. Although the mode in 4-phenylbenzaldehyde is not a pure hydrogen bond stretching, as it also involves the ring slipping of pi-stacking dimers, it falls in the expected wavenumber range for the $\text{CH}\cdots\text{O}$ interaction.

3. Materials and Methods

4-Phenylbenzaldehyde was obtained commercially (Sigma–Aldrich, CAS number 459-57-4) and used as supplied.

The ATR-FTIR spectra of solid 4-phenylbenzaldehyde (Figure S1, Supplementary Materials) was measured on a Vertex 70 spectrometer using a Platinum ATR single reflection diamond accessory. For the far-IR spectrum ($50\text{--}600\text{ cm}^{-1}$) a silicon solid-state beam-splitter and a Deuterated L-alanine doped TriGlycine Sulphate (DLaTGS) detector with a polyethylene window was used. The mid-IR spectrum ($400\text{--}4000\text{ cm}^{-1}$) was recorded using a Ge on KBr substrate beam-splitter and a liquid nitrogen cooled wide band mercury cadmium telluride (MCT) detector. All spectra were the average of two counts of 128 scans each. A spectral resolution of 2 cm^{-1} was used.

The Raman spectrum was recorded on a Jobin-Yvon T64000 spectrometer, in the subtractive mode configuration, using a 514.5 nm argon ion laser line, a non-intensified charge coupled device (CCD) detector, with an integration time of 5 s. The resolution was approximately 3 cm^{-1} and the estimated error in wavenumber was less than 1 cm^{-1} .

INS spectrum: the inelastic neutron scattering experiment was performed with the TOSCA spectrometer, an indirect geometry time-of-flight spectrometer at the ISIS Neutron and Muon Source at the Rutherford Appleton Laboratory (Chilton, UK). The sample, with a total amount of ca. 2 g, was packed inside a flat thin-walled aluminum can of 4.8 cm height and 4 cm width, with a path length of 2 mm, which was mounted perpendicular to the beam, using a regular TOSCA centre-stick. The spectrum was collected below 15 K, measured for the $16\text{--}8000\text{ cm}^{-1}$ energy-transfer range, and the resolution was $\Delta E/E \approx 1.5\%$.

Quantum chemistry calculations: single molecule (discrete) calculations were performed with Gaussian 09 program (G09), version A.02 [37] using the PBE pure density functional combined with the 6-311G(d,p) basis set, as implemented in G09. Frequency calculations, subsequent to full geometry optimization, provide the infrared and Raman intensities and confirm the convergence to a true minimum (no imaginary frequencies). Potential energy functions for internal rotations have been obtained through the “scan” option (OPT = ModRedundant keyword) of G09, using the step size of 10° .

Periodic density functional theory (periodic-DFT) calculations were carried out using the plane-wave/pseudopotential method as implemented in the CASTEP code [17,38]. Exchange and correlation were approximated using the PBE functional [39]. The plane-wave cut-off energy was 830 eV. Brillouin zone sampling of electronic states was performed on the $8 \times 4 \times 4$ Monkhorst-Pack grid.

The equilibrium structure, an essential prerequisite for lattice dynamics calculations was obtained by LBFGS geometry optimization after which the residual forces were converged to zero within $0.005\text{ eV}\cdot\text{\AA}^{-1}$. The initial structure was taken from the reported crystal structure (CSD entry: WASLOS), and the cell parameters were kept constant during geometry optimization. This is important when using standard GGA functions, as their description of dispersion/van der Waals interactions is defective, leading to unrealistic cell dimensions. Phonon frequencies were obtained by the diagonalization of dynamical matrices computed using the density-functional perturbation theory. The eigenvectors (atomic displacements) for each normal mode that are part of the CASTEP output, enable visualization of the modes to aid assignments and are also all that is required to generate the INS spectrum using the program aClimax [40]. Program aClimax calculates INS intensities incorporating the instrumental

bandwidth in a calculated spectrum that is easily compared with the experiment. It is emphasized that for all the calculated spectra shown the transition energies were not scaled.

Visualization of the atomic displacements of vibrational modes was performed using the Jmol program [41].

The determination of the potential barrier for a single simple internal rotor from torsional transitions has been performed with the program Barrier [26]. For an estimated error in torsional frequencies of less than 2 cm^{-1} , the error in the barrier height was ca. 3%.

4. Conclusions

The present work is a simple exercise that illustrates the capabilities of periodic DFT as an aid in the vibrational assignment of organic crystals. Despite being more resource intensive than its discrete counterparts, the effort of running periodic DFT calculations pays off by delivering accurate estimated spectra, which can be used as a direct guide for assignments. Even though 4-phenylbenzaldehyde individual units are held together by weak C-H \cdots O and pi-stacking interactions—therefore a prime candidate for the “cheaper” discrete model approach—a periodic description is necessary for reproducing the full vibrational features. An example of the latter is the phenyl torsion, whose frequency is severely underestimated by the single molecule approach, misleading its assignment. From the corrected torsional frequency, the torsional barrier value of $V_4 = 2600\text{ cm}^{-1}$ was obtained for the phenyl group, well above the value of $V_4 = 860\text{ cm}^{-1}$ predicted for the isolated molecule. This contrasts with the torsional barrier of the aldehyde group, -CHO, which was clearly less affected by crystal packing (4000 cm^{-1} vs. 3600 cm^{-1} , for the crystal and isolated molecule, respectively). In addition, periodic DFT is fundamental for understanding the low wavenumber region of INS spectra, offering a bird’s-eye view of collective modes such as the antitranslational motion of CH \cdots O bonded pairs, a hallmark vibrational mode of systems where C-H \cdots O contacts are an important feature.

Supplementary Materials: The following are available online, Figure S1: Mid Infrared spectrum of 4-phenylbenzaldehyde in the 400–4000 cm^{-1} range (top), compared with the CASTEP calculated spectrum (bottom). Table S1: Coordinates of the optimized structure of 4-phenylbenzaldehyde (G09, PBEPBE/6-311G(d,p) keyword).

Author Contributions: Formal analysis, P.R.-C.; investigation, M.M.N. (INS, CASTEP), C.F.A. (G09), P.D.V. (INS), A.M.A. (Raman, Far-IR); writing—original draft preparation, M.M.N.; writing—review and editing, M.M.N., P.R.-C., C.F.A., P.D.V.; supervision, P.R.-C.; funding acquisition, P.R.-C. All authors have read and agreed to the published version of the manuscript.

Funding: This work was developed within the scope of the project CICECO-Aveiro Institute of Materials, UIDB/50011/2020 & UIDP/50011/2020, financed by national funds through the FCT/MEC and when appropriate co-financed by FEDER under the PT2020 Partnership Agreement. A.M.A. acknowledges financial support given by POCentro, COMPETE 2020, Portugal 2020, European Community through the FEDER and FCT to Unidade de I&D Química-Física Molecular of the University of Coimbra (UIDB/00070/2020). FCT is gratefully acknowledged for funding a PhD grant to C.F.A. (SFRH/BD/129040/2017) and a researcher contract to M.M.N. (IF/01468/2015) under the program IF 2015.

Acknowledgments: The STFC Rutherford Appleton Laboratory is thanked for access to neutron beam facilities. CASTEP calculations were made possible due to the computing resources provided by STFC Scientific Computing Department’s SCARF cluster.

Conflicts of Interest: The authors declare no conflict of interest.

References

1. Araujo, C.; Freire, C.S.R.; Nolasco, M.M.; Ribeiro-Claro, P.J.A.; Rudić, S.; Silvestre, A.J.D.; Vaz, P.D. Hydrogen Bond Dynamics of Cellulose through Inelastic Neutron Scattering Spectroscopy. *Biomacromolecules* **2018**, *19*, 1305–1313. [[CrossRef](#)] [[PubMed](#)]
2. Ribeiro-Claro, P.J.A.; Vaz, P.D.; Nolasco, M.M.; Amado, A.M. Understanding the vibrational spectra of crystalline isoniazid: Raman, IR and INS spectroscopy and solid-state DFT study. *Spectrochim. Acta Part A Mol. Biomol. Spectrosc.* **2018**, *204*, 452–459. [[CrossRef](#)]

3. Parker, S.F.; Butler, I.R. Synthesis, Computational Studies, Inelastic Neutron Scattering, Infrared and Raman Spectroscopy of Ruthenocene. *Eur. J. Inorg. Chem.* **2019**, *2019*, 1142–1146. [[CrossRef](#)]
4. Ribeiro-Claro, P.J.; Vaz, P.D.; Nolasco, M.M.; Araujo, C.F.; Gil, F.P.S.C.; Amado, A.M. Vibrational dynamics of 4-fluorobenzaldehyde from periodic DFT calculations. *Chem. Phys. Lett. X* **2019**, *2*, 100006. [[CrossRef](#)]
5. Bilski, P.; Druzbicki, K.; Jencyk, J.; Mielcarek, J.; Wasicki, J. Molecular and Vibrational Dynamics in the Cholesterol-Lowering Agent Lovastatin: Solid-State NMR, Inelastic Neutron Scattering, and Periodic DFT Study. *J. Phys. Chem. B* **2017**, *121*, 2776–2787. [[CrossRef](#)] [[PubMed](#)]
6. Sahoo, S.; Ravindran, T.R.; Chandra, S.; Sarguna, R.M.; Das, B.K.; Sairam, T.N.; Sivasubramanian, V.; Thirimal, C.; Murugavel, P. Vibrational spectroscopic and computational studies on diisopropylammonium bromide. *Spectrochim. Acta Part A Mol. Biomol. Spectrosc.* **2017**, *184*, 211–219. [[CrossRef](#)]
7. Ding, L.; Fan, W.-H.; Chen, X.; Chen, Z.-Y.; Song, C. Terahertz spectroscopy and solid-state density functional theory calculations of structural isomers: Nicotinic acid, isonicotinic acid and 2-picolinic acid. *Mod. Phys. Lett. B* **2017**, *31*. [[CrossRef](#)]
8. Druzbicki, K.; Mielcarek, J.; Kiwilsza, A.; Toupet, L.; Collet, E.; Pajzderska, A.; Wasicki, J. Computationally Assisted (Solid-State Density Functional Theory) Structural (X-ray) and Vibrational Spectroscopy (FT-IR, FT-RS, TDs-THz) Characterization of the Cardiovascular Drug Lacidipine. *Cryst. Growth Des.* **2015**, *15*, 2817–2830. [[CrossRef](#)]
9. Bec, K.B.; Grabska, J.; Czarnecki, M.A.; Huck, C.W.; Wojcik, M.J.; Nakajima, T.; Ozaki, Y. IR Spectra of Crystalline Nucleobases: Combination of Periodic Harmonic Calculations with Anharmonic Corrections Based on Finite Models. *J. Phys. Chem. B* **2019**, *123*, 10001–10013. [[CrossRef](#)]
10. Pawlukoć, A.; Hetmańczyk, Ł. INS, DFT and temperature dependent IR studies on dynamical properties of acetylcholine chloride. *Vib. Spectrosc.* **2016**, *82*, 37–43. [[CrossRef](#)]
11. Druzbicki, K.; Mikuli, E.; Pałka, N.; Zalewski, S.; Ossowska-Chruściel, M.D. Polymorphism of Resorcinol Explored by Complementary Vibrational Spectroscopy (FT-RS, THz-TDS, INS) and First-Principles Solid-State Computations (Plane-Wave DFT). *J. Phys. Chem. B* **2015**, *119*, 1681–1695. [[CrossRef](#)] [[PubMed](#)]
12. Zhong, L.; Parker, S.F. Structure and vibrational spectroscopy of methanesulfonic acid. *R. Soc. Open Sci.* **2018**, *5*. [[CrossRef](#)] [[PubMed](#)]
13. Deringer, V.L.; George, J.; Dronskowski, R.; Englert, U. Plane-Wave Density Functional Theory Meets Molecular Crystals: Thermal Ellipsoids and Intermolecular Interactions. *Acc. Chem. Res.* **2017**, *50*, 1231–1239. [[CrossRef](#)] [[PubMed](#)]
14. Kresse, G.; Furthmüller, J. Efficiency of ab-initio total energy calculations for metals and semiconductors using a plane-wave basis set. *Comput. Mater. Sci.* **1996**, *6*, 15–50. [[CrossRef](#)]
15. Dovesi, R.; Erba, A.; Orlando, R.; Zicovich-Wilson, C.M.; Civalieri, B.; Maschio, L.; Rerat, M.; Casassa, S.; Baima, J.; Salustro, S.; et al. Quantum-mechanical condensed matter simulations with CRYSTAL. *WILEY Interdiscip. Rev. Mol. Sci.* **2018**, *8*, e1360. [[CrossRef](#)]
16. Dovesi, R.; Saunders, V.R.; Roetti, C.; Orlando, R.; Zicovich-Wilson, C.M.; Pascale, F.; Civalieri, B.; Doll, K.; Harrison, N.M.; Bush, I.J.; et al. *CRYSTAL17 User's Manual 2017*; University of Torino: Torino, Italy, 2017.
17. Clark, S.J.; Segall, M.D.; Pickard, C.J.; Hasnip, P.J.; Probert, M.J.; Refson, K.; Payne, M.C. First principles methods using CASTEP. *Zeitschrift Fur Krist.* **2005**, *220*, 567–570. [[CrossRef](#)]
18. Pawlukoć, A.; Hołderna-Natkaniec, K.; Bator, G.; Natkaniec, I. L-glutamine: Dynamical properties investigation by means of INS, IR, RAMAN, 1H NMR and DFT techniques. *Chem. Phys.* **2014**, *443*, 17–25. [[CrossRef](#)]
19. Kearley, G.J. A review of the analysis of molecular vibrations using INS. *Nucl. Instruments Methods Phys. Res. Sect. A.* **1995**, *354*, 53–58. [[CrossRef](#)]
20. Verdal, N.; Hudson, B.S. Inelastic neutron scattering and periodic DFT studies of crystalline aromatic materials: Biphenylene—A Mills-Nixon molecule. *Chem. Phys. Lett.* **2007**, *434*, 241–244. [[CrossRef](#)]
21. Vaz, P.D.; Nolasco, M.; Fonseca, N.; Amado, A.M.; Amorim Da Costa, A.M.; Félix, V.; Drew, M.G.B.; Goodfellow, B.J.; Ribeiro-Claro, P.J.A. C-H...O hydrogen bonding in 4-phenyl-benzaldehyde: A comprehensive crystallographic, spectroscopic and computational study. *Phys. Chem. Chem. Phys.* **2005**, *7*, 3027–3034. [[CrossRef](#)]
22. Srishailam, K.; Reddy, B.V.; Rao, G.R. Investigation of torsional potentials, hindered rotation, molecular structure and vibrational properties of some biphenyl carboxaldehydes using spectroscopic techniques and density functional formalism. *J. Mol. Struct.* **2019**, *1196*, 139–161. [[CrossRef](#)]

23. Nolasco, M.M.; Amado, A.M.; Ribeiro-Claro, P.J.A. Computationally-assisted approach to the vibrational spectra of molecular crystals: Study of hydrogen-bonding and pseudo-polymorphism. *ChemPhysChem* **2006**, *7*, 2150–2161. [[CrossRef](#)] [[PubMed](#)]
24. Mendes, N.F.C.; Nolasco, M.M.; Ribeiro-Claro, P.J.A. Effects of hydrogen-bond and cooperativity in the vibrational spectra of Luminol. *Vib. Spectrosc.* **2013**, *64*, 119–125. [[CrossRef](#)]
25. Sardo, M.; Amado, A.M.; Ribeiro-Claro, P.J.A. Hydrogen bonding in nitrofurantoin polymorphs: A computation-assisted spectroscopic study. *J. Raman Spectrosc.* **2009**, *40*, 1956–1965. [[CrossRef](#)]
26. Groner, P. *Barrier*, version 22; University of Missouri: Kansas City, MO, USA, 2019.
27. Godunov, I.A.; Bataev, V.A.; Abramnikov, A.V.; Pupyshev, V.I. The Barriers to Internal Rotation of Benzaldehyde and Benzoyl Fluoride: “Reconciliation{”} Between Theory and Experiment. *J. Phys. Chem. A* **2014**, *118*, 10159–10165. [[CrossRef](#)]
28. Araujo, C.F.; Nolasco, M.M.; Ribeiro-Claro, P.J.A.; Rudić, S.; Silvestre, A.J.D.; Vaz, P.D.; Sousa, A.F. Inside PEF: Chain Conformation and Dynamics in Crystalline and Amorphous Domains. *Macromolecules* **2018**, *51*, 3515–3526. [[CrossRef](#)]
29. Kurapov, P.B.; Klyuev, N.A.; Tyulin, V.I. Potential function of inner rotation of diphenyl. *Theor. Exp. Chem.* **1988**, *24*, 190–197. [[CrossRef](#)]
30. Tylli, H.; Konschin, H. Raman-spectroscopic study of low frequency vibrations in anisole and anisole-d3. *J. Mol. Struct.* **1977**, *42*, 7–12. [[CrossRef](#)]
31. Chiang, W.Y.; Laane, J. Fluorescence-spectra and torsional potential functions for trans-stilbene in its S0 and S1 (π,π^*) electronic states. *J. Chem. Phys.* **1994**, *100*, 8755–8767. [[CrossRef](#)]
32. Chiang, W.Y.; Laane, J. Fluorescence-spectra and torsional potential energy functions for 4-methoxy-trans-stilbene in its S0 and S1 (π,π^*) electronic states. *J. Phys. Chem.* **1995**, *99*, 11823–11829. [[CrossRef](#)]
33. Vaz, P.D.; Nolasco, M.M.; Gil, F.P.S.C.; Ribeiro-Claro, P.J.A.; Tomkinson, J. Hydrogen-bond dynamics of C-H \cdots O interactions: The chloroform \cdots acetone case. *Chem. A Eur. J.* **2010**, *16*, 9010–9017. [[CrossRef](#)] [[PubMed](#)]
34. Vaz, P.D.; Nolasco, M.M.; Ribeiro-Claro, P.J.A. Intermolecular C-H center dot center dot center dot O interactions in cyclopentanone: An inelastic neutron scattering study. *Chem. Phys.* **2013**, *427*, 117–123. [[CrossRef](#)]
35. Li, J.C.; Ross, D.K. Evidence for two kinds of hydrogen bond in ice. *Nature* **1993**, *365*, 327–329. [[CrossRef](#)]
36. Corsaro, C.; Crupi, V.; Longo, F.; Majolino, D.; Venuti, V.; Wanderlingh, U. Mobility of water in Linde type A synthetic zeolites: An inelastic neutron scattering study. *J. Phys. -Condens. Matter* **2005**, *17*, 7925–7934. [[CrossRef](#)]
37. Frisch, M.J.; Trucks, G.W.; Schlegel, H.B.; Scuseria, G.E.; Robb, M.A.; Cheeseman, J.R.; Scalmani, G.; Barone, V.; Mennucci, B.; Petersson, G.A.; et al. *Gaussian 09, Revision A.02*; Gaussian, Inc.: Wallingford, CT, USA, 2009.
38. Refson, K.; Tulip, P.R.; Clark, S.J. Variational density-functional perturbation theory for dielectrics and lattice dynamics. *Phys. Rev. B* **2006**, *73*, 155114. [[CrossRef](#)]
39. Perdew, J.P.; Burke, K.; Ernzerhof, M. Generalized gradient approximation made simple. *Phys. Rev. Lett.* **1996**, *77*, 3865–3868. [[CrossRef](#)]
40. Ramirez-Cuesta, A.J. aCLIMAX 4.0.1, The new version of the software for analyzing and interpreting INS spectra. *Comput. Phys. Commun.* **2004**, *157*, 226–238. [[CrossRef](#)]
41. *Jmol: An Open-Source Java Viewer for Chemical Structures in 3D*; Jmol Development Team: Minneapolis, MN, USA, 2016; Available online: <http://jmol.sourceforge.net/> (accessed on 24 February 2020).

Sample Availability: Samples of the compounds are not available from the authors.



© 2020 by the authors. Licensee MDPI, Basel, Switzerland. This article is an open access article distributed under the terms and conditions of the Creative Commons Attribution (CC BY) license (<http://creativecommons.org/licenses/by/4.0/>).